J. Condensed Matter Nucl. Sci. 39 (2025) 322–345

Research Article

$\sqrt[3]{A}$—Law in Nuclear Transmutation of Metal Hydrides

X. Z. Li, C. L. Liang, G. S. Huang, B. Liu, J. Tian, S. Chen,
Y. Chen, Z. M. Dong

Dept. of Physics, Tsinghua University, Beijing, China

S. X. Zheng

Dept. of Engineering Physics, Tsinghua University, Beijing, China

Abstract

2-step resonance model is proposed to combine the resonance with Bethe's solar energy model and Oppenheimer's stripping reaction model. It is able to explain both the $\sqrt[3]{A}$–law (the atomic-mass-number (A)-dependence of transmutation rate) and the Arrhenius plot (the temperature dependence of excess power) in the metal-hydrides experiments. The pull-in effect of the resonance may pull two charged nuclei together even if the kinetic energy is much lower than the height of Coulomb barrier. The K-electron capture in lattice is more favorable than the positron emission, there by suppresses the Gamma radiation in metal-hydride experiments. The Oppenheimer stripping reaction is more favorable to the proton emission, there by suppresses the neutron radiation as well. 2 steps are necessary to develop first a perfect elastic scattering without any damping, then the second inelastic process is greatly enhanced by this resonance. The pull-in effect makes the resonance height even higher at even lower energy. Hence, the resonance integration does not vanish when the width of the resonance is very narrow at low energy because the energy dependence of the phase-shift at low energy keeps the resonance integration finite. This important energy dependence of the phase-shift is extracted from the experimental data in Appendix. This model is further applied to the case of electron screening experiments and explains the 5-peak pattern in the electron screening potentials using $\sqrt[3]{A}$–law again. If the proposed electron screening experiment using enriched isotope as the screening material shows that there is an isotope effect: i.e. same atomic number (Z) with different atomic mass number (A) would have different electron screening potential, then the nuclear nature involved in the electron screening potential would be revealed. As a result, the lattice is not a house to burn H(D), but a burning house in H(D) with resonance.

Keywords: 2-step resonance model, Bethe's solar energy model, Oppenheimer's stripping reaction model, Arrhenius plot of excess power, cubic-root-law of atomic mass number, 5-peak pattern in A-dependence, Pull-in effect of the resonance, isotope effect in electron screening potential, energy dependence of phase-shift at low energy, a new simple formula for fusion cross-section of light nuclei.

© 2025 ICCF. All rights reserved. ISSN 2227-3123

1. Introduction

After 34 years of exploration, the regularity in the experimental data from various laboratories all over the world offers compelling evidence showing that condensed matter nuclear science is real. The temperature (T)-dependence of the excess power has appeared everywhere consistently, and the atomic mass number (A)-dependence of the production rate of the new nuclides in the metal-H (D) system has similar peak pattern consistently, as well. Moreover, these regularities might be further expressed in a quantitative way: i.e., 6 straight lines in temperature dependence (T), and more straight lines in cubic-root of atomic mass number ($\sqrt[3]{A}$) dependence were presented in ICCF-21, ICCF-22, and in ICCF-24 [1]–[3]. Based on these straight lines, a 2-step resonance model has been proposed. This model is able to explain both the T-dependence in excess heat and $\sqrt[3]{A}$-dependence in nuclear transmutation. Unexpectedly, this model is able to explain the peak pattern in the electron screening data from hot fusion experiments as well. This paper attempts to show how this 2-step resonance model is able to derive the T-dependence in excess power and the $\sqrt[3]{A}$-dependence in nuclear transmutation. The $\sqrt[3]{A}$-dependence in electron screening potential would provide further a test to the 2-step resonance model. The proposed test for the isotope effect of the "electron" screening would reveal the nuclear nature of the electron screening, and provide additional evidence for the low energy nuclear resonance.

2. Conceptual Hints From Experimental Data—Elastic Feature of an Inelastic Process and Peaks in Nuclear Transmutation

During the ARPA-E workshop (2021) D. Nagel showed two plots for excess heat and for nuclear transmutation [4]. In Fig. 1, the log of excess power is plotted against (1/T(Kelvin)). Three straight lines are typical behavior for a diffusion process. The diffusion process is an elastic scattering process; however, the excess power is from an inelastic process. It implies that the excess power must be produced in a 2-step reaction.

In ICCF-21 (2018), a 2-step resonance model was proposed to derive these straight lines in the semi-logarithmic plot [1]. In ICCF-22 (2019), 3 more straight lines were found to support this 2-step resonance model [2]. In ICCF-23 (2022) we attempted to use the same model to explain the peak pattern in the nuclear transmutation of metal hydrides [3].

In Fig. 2a, the production rate of new nuclide is plotted against the atomic mass number A, the distances between the five peaks are not equal. However, if we plot the same picture against the cubic root of A ($\sqrt[3]{A}$); then, the distances

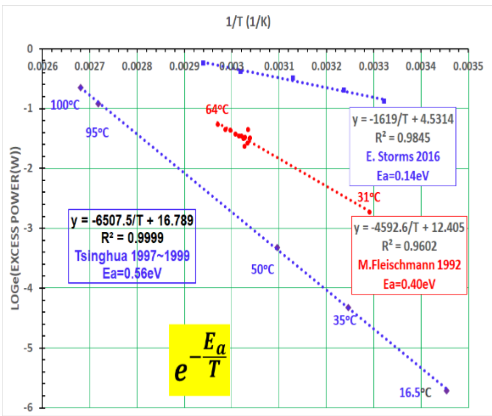

Figure 1. 3 straight lines imply a 2-step model.

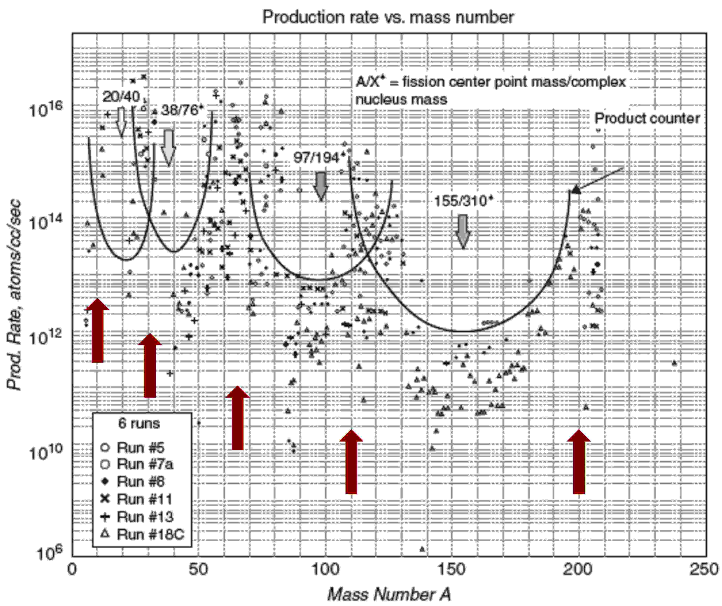

Figure 2a. Production rate versus A.

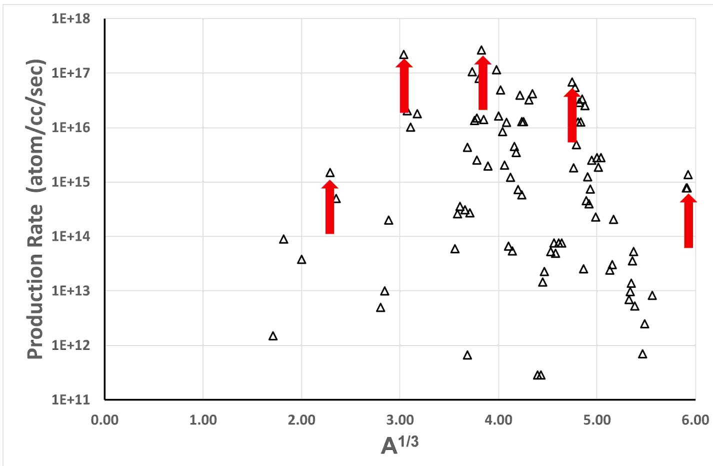

Figure 2b. Production rate versus $\sqrt[3]{A}$ implies a resonance process involved.

between the five red arrows are almost equal (Fig. 2b). In Fig. 2b only Run #8 and #18C are selected to locate the peak's position for Ni-H data on glass beads only (other data points in Fig. 2a, include the data from Pd-H layer and plastic beads). The periodicity in the cubic root of A ($\sqrt[3]{A}$) is evident. Since the size of a nucleus is proportional to the

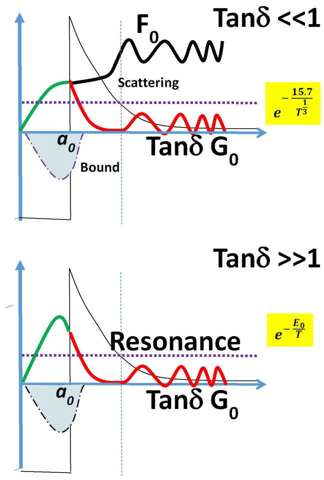

Figure 3. Bethe's solar energy model is extended to the case of Tanδ>>1 for LENR.

cubic root of the atomic mass number ($\sqrt[3]{A}$), this periodicity implies that the aforementioned inelastic process might be related to the nuclear resonance.

3. 2-Step Resonance Model—the Extension of Bethe's Solar Energy Model

Bethe proposed that p-p elastic scattering produces an initial state for a transition to the final state (i.e., d-n bound state). The weak interaction was proposed to change a proton into a neutron [5]. The probability of this transition depends on the overlapping between the initial wave function and the final wave function. Bethe found that even if in the case of non-resonance the resonance branch $Tan\delta \cdot G_0$ (red solid line in Fig. 3) in the wave function of the initial state played the same important role as that of the non-resonance branch F_0 (thick black line in Fig. 3) in the overlapping. Bethe called this as "resonance effect in the case of non-resonance." We shall show first how this overlapping leads to the Gamow peak behavior in the non-resonance case; then, how this overlapping would lead to the straight line in a semi-logarithmic plot in the resonance case.

3.1. The Resonance Effect in the Case of a Non-Resonance—Gamow Peak for Hot Fusion

Bethe assumed that a Coulomb field is connected to a square nuclear potential well as shown by thin black solid line in Fig. 3. The solution of the S-wave equation in the Coulomb field is a linear combination of the resonance branch (G_0) and the non-resonance branch (F_0). The coefficient of this linear combination is $Tan[\delta]$. Here δ is the phase-shift for S-wave. Since there is no low energy resonance for p-p elastic scattering, $Tan[\delta]$ is a very small number ($\sim$0.0017 for Bethe's case). However, the resonance term ($Tan[\delta]G_0$) there is still not negligible because $G_0[r_0] \propto \theta$ approaches a big number near the nuclear surface ($r = a_0$) and ($Tan[\delta]G_0$) is still comparable with $F_0[r_0] \propto \frac{1}{\theta}$ which is a small number. Thus, both the resonance branch and the non-resonance branch in the initial wave function will have similar contribution to the overlapping with the final wave function, because the final wave function is extended outside the nuclear surface only a little distance (the black dash-dotted line in Fig. 3) and it makes overlapping sensitive to the value of the initial wave function near the nuclear surface only.

Here, $\theta \equiv \sqrt{\frac{e^{2\pi\eta}-1}{2\pi}}$; $\eta \equiv \frac{1}{ka_c}$; $k = \sqrt{\frac{2\mu E}{\hbar^2}}$; $\hbar$ is the Planch constant divided by 2π; μ is the reduced mass; E is the kinetic energy in CM system; $a_c = \frac{4\pi\epsilon_0\hbar^2}{\mu e^2}$ is the length of the Coulomb unit; e is the electric charge of a proton, ϵ_0 is the dielectric constant of vacuum. When energy E is increasing, θ is decreasing with E very fast; therefore, $\frac{1}{\theta}$ increases very fast. On the other hand, Boltzmann factor, $e^{-\frac{E}{T}}$, decreases very fast when E is increases at low temperature (T). As a result, when we integrate over energy, E, to calculate the average reaction rate over Maxwell distribution of velocity of proton, $< \sigma\ v > \propto \left(\frac{1}{\theta}\right)^2 e^{-\frac{E}{T}}$ will have a very sharp peak (i.e., Gamow peak). This integration may be calculated using the steepest descent method, and obtain the famous Gamow temperature dependence, $e^{-\frac{15.7}{T^{1/3}}}$. Here, T is the proton-plasma temperature in unit of *keV*. This is why hot fusion people tried to make plasma temperature as high as *keV*.

3.2. The Resonance Effect in the Case of Resonance—Straight Line in Semi-Logarithmic Plot for Cold Fusion

The phase-shift $\delta = \frac{\pi}{2}$ in the case of resonance. This leads to two important changes in Bethe's calculation which would dramatically change the temperature dependence of the reaction rate, and would give a straight line in semi-logarithmic plot.

(1) Bethe's approximation, $e^{i\delta}Cos[\delta] \sim 1$, is no longer valid. The initial wave function in the Coulomb field should be rewritten as:

$$\begin{aligned} e^{i\delta}\mathrm{Cos}\,[\delta]\,(F_0 + Tan\,[\delta]\,G_0) &= e^{i\delta}\,(\mathrm{Cos}\,[\delta]\,F_0 + Sin\,[\delta]\,G_0) \\ &= e^{i\delta}\left(\frac{Cot[\delta]}{\sqrt{1+Cot[\delta]^2}}F_0 + \frac{1}{\sqrt{1+Cot[\delta]^2}}G_0\right) \end{aligned} \tag{1}$$

(2) Bethe's approximation, $\mathrm{Tan}\,[\delta] \sim \frac{1}{\theta^2} * Constant$, should be replaced by:

$$\mathrm{Tan}\,[\delta] = -\left.\frac{F_0}{G_0}\frac{\frac{1}{w}\frac{\partial w}{\partial r} - \frac{1}{F_0}\frac{\partial F_0}{\partial r}}{\frac{1}{w}\frac{\partial w}{\partial r} - \frac{1}{G_0}\frac{\partial G_0}{\partial r}}\right]_{r=a_0} = \frac{1}{\theta^2}\frac{1}{(C_1 + C_2E)}, \tag{2}$$

Here, $\left.\frac{1}{w}\frac{\partial w}{\partial r}\right]_{r=a_0}$ is the logarithmic derivative of the wave function at the nuclear inner surface. When the denominator of Eq. (2),

$$\left.\left[\frac{1}{w}\frac{\partial w}{\partial r} - \frac{1}{G_0}\frac{\partial G_0}{\partial r}\right]\right|_{r=a_0} = 0, \tag{3}$$

$\delta = \frac{\pi}{2}$. There will be a resonance. However, the exact behavior of $\left.\left[\frac{F_0}{G_0}\frac{\frac{1}{w}\frac{\partial w}{\partial r} - \frac{1}{F_0}\frac{\partial F_0}{\partial r}}{\frac{1}{w}\frac{\partial w}{\partial r} - \frac{1}{G_0}\frac{\partial G_0}{\partial r}}\right]\right|_{r=a_0}$ is unknown. It has to be determined by the experimental data only. After 30 years of pursuing this question, we found that 24 pairs of low energy nuclear fusion data available from National Nuclear Data Center [6] might be fit by

$$-\left.\left[\frac{F_0}{G_0}\frac{\frac{1}{w}\frac{\partial w}{\partial r} - \frac{1}{F_0}\frac{\partial F_0}{\partial r}}{\frac{1}{w}\frac{\partial w}{\partial r} - \frac{1}{G_0}\frac{\partial G_0}{\partial r}}\right]\right]_{r=a_0} \approx \frac{1}{\theta^2}\frac{1}{C_1 + C_2E + i\,C_3}, \tag{4}$$

Here, C_1, C_2 and C_3 are 3 fitting constants [7]–[10] (see Appendix A). For the case of elastic scattering, $C_3 = 0$; and $E_0 = -\frac{C_1}{C_2}$, when $\left.\left[\frac{1}{w}\frac{\partial w}{\partial r} - \frac{1}{G_0}\frac{\partial G_0}{\partial r}\right]\right|_{r=a_0} = 0$ at $E = E_0$. Therefore, when we integrate

$\left|\frac{1}{\sqrt{1+Cot[\delta]^2}}G_0\right|^2 e^{-\frac{E}{T}}$, over the energy, E, to obtain the average reaction rate, $< \sigma v >$, near the resonance we will have a very sharp peak for $\left|\frac{1}{\sqrt{1+Cot[\delta]^2}}G_0\right|^2$ at $E = E_0$, because $\left|\frac{1}{\sqrt{1+Cot[\delta]^2}}G_0\right|^2_{r=a_0} \approx \frac{\theta^2}{1+\theta^4(C_2(E-E_0))^2}$. It acts like a delta function in the integration: it is very large as θ^2, at $E = E_0$, and it approaches to $\frac{1}{\theta^2} \to 0$ quickly when E is away from E_0. So the integration of $\left|\frac{1}{\sqrt{1+Cot[\delta]^2}}G_0\right|^2 e^{-\frac{E}{T}}$ would evaluate the $e^{-\frac{E}{T}}$ at $E = E_0$ only, i.e. $e^{-\frac{E_0}{T}}$. This is just the straight line in semi-logarithmic plot in Fig. 1 which was discovered by E. Storms in 2016 [11]. Indeed, Storms' discovery just confirms the existence of the low energy resonance in cold fusion. Now we may try to find the $\sqrt[3]{A}$—Law using this resonance condition Eq. (3).

4. The Equation—the Boundary Condition Selects the Resonant Branch

Equation (3) is the necessary condition for the nuclear wave function to have a smooth connection to a resonance branch of the Coulomb wave function at the nuclear boundary. When the logarithmic derivative of the wave function at the inner surface of the nuclear potential well, $\frac{1}{w}\frac{\partial w}{\partial r}\Big]_{r=a_0}$, is just equal to that of the resonant branch of the wave function, $\frac{1}{G_0}\frac{\partial G_0}{\partial r}\Big]_{r=a_0}$, in the Coulomb field, $\mathrm{Cot}\,[\delta] \to 0$. Then only the resonant branch, G_0 , remains in the linear combination (Eq. (1)). In this case, the wave function will peak at the interface. This implies that 2 positively charged nuclei may stay close together even if inside a Coulomb field. Or we may say that the nuclear resonance delivers a positive charged nucleus to the surface of another positively charged nucleus (the pull-in effect of a resonance). This smooth connection condition is an equation for the radius of nuclear potential well, a_0. Hence, we may find the $\sqrt[3]{A}$–law using this resonance condition. Equation (3) may be rewritten to show its dependence on $\sqrt[3]{A}$ as:

$$k_1 \mathrm{Cot}\,[k_1 a_0] = -\sqrt{\frac{2}{a_0 a_c}} \tag{5}$$

$$a_0 = c_{\mathrm{a}}\,(\sqrt[3]{A} + 1) \tag{6}$$

Here, k_1 is the wave number inside the nuclear potential well, A is the atomic mass number of the target nucleus—the reactant which is interacting with a proton, c_{a} is a constant. The right-hand-side of Eq. (5) is from the mathematical handbook for Coulomb wave function, G_0 [12]. Its value is in the order of 10^{14} m^{-1}. The k_1 in the left-hand-side of Eq. (5) is in the order of 10^{15} m^{-1}; therefore, $\mathrm{Cot}\,[k_1 a_0]$ must be small, and $k_1 a_0$ must be a little greater than $\frac{\pi}{2}$(2N+1). Here, N is an integer. For the metal with charge number *Z*.

$$-k_1\left(k_1 a_0 - \frac{\pi}{2}(2N+1)\right) = -\sqrt{\frac{2}{c_{\mathrm{a}}\,(\sqrt[3]{A}+1)\frac{4\pi\epsilon_0\hbar^2}{\mu Z e^2}}} \tag{7}$$

The right hand-side of Eq. (7) is a function of $\sqrt[3]{A}$ as well, and may be numerically approximated by (1.22 $\sqrt[3]{A}$–0.469) $\times 10^{14} m^{-1}$. So both sides are the linear function of $\sqrt[3]{A}$, and show its periodicity already. Using the parameters from the nuclear optical model, the depth of nuclear potential well is: $U_{\mathrm{optical}} = 53.3\ MeV$ and $c_{\mathrm{a}} = 1.746 \times 10^{-15} m$ [8], [13], we may further to obtain the coefficients in the $\sqrt[3]{A}$ -law:

$$\sqrt[3]{A_N} = 1.13\ N - 0.46. \tag{8}$$

A_N is the atomic mass number corresponding *t*o the N-th peak based on 2-step resonance model. These coefficients may be compared with Miley's Ni-H experiments in 1996 [14]; however, we should not compare directly with 5 peaks in Fig. 2a.

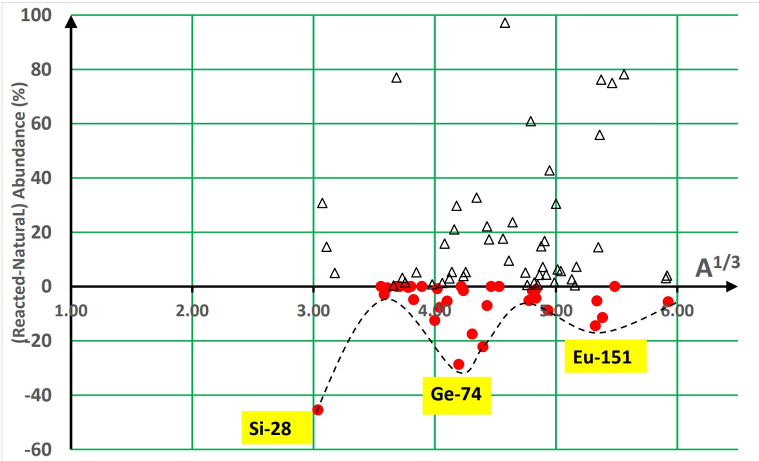

Figure 4. Miley's 3 depletion peaks with equal distance in $\sqrt[3]{A}$ scale.

5. Comparison With Experiment—Reactant's Atomic Mass Number Is Needed for Comparison

The atomic mass number in equation (6) is for the reactant, not for the product of nuclear transmutation, because in equation (6), A is the atomic mass number for the reactant—the target nucleus. Hence, Figure 2a is not the right data for comparison because Fig. 2a is for atomic mass number of the nuclear product, not for the reactant. We have to find the atomic mass number for the reactant. Fortunately, Miley's experiment lasted 2 weeks long. The nuclear products of nuclear transmutation were still in the hydrogen environment. If any isotope was interacting with a proton, this isotope would be a reactant and it would be depleted. So, any depletion peak in isotope abundance gives the peak atomic mass number for the reactant. Based on Miley's data for Ni-H system (Run # 8) [14], we plot the deviation of the isotope abundance from the natural abundance in Fig. 4. All depleted isotopes are in red solid circles. In the scale of $\sqrt[3]{A}$, we have three peaks in equal distance at Eu-151, Ge-74, and Si-28. Using these 3 atomic mass numbers, we have the $\sqrt[3]{A}$ –law again in Fig. 5 with the coefficient of determination, $R^2 = 0.9999$ (R^2 is a measurement of the fitting. $R^2 = 1$, when 3 points are on a straight line perfectly)

$$\sqrt[3]{A_N} = 1.1442\ N - 0.3903, \quad (N = 3,\ 4,\ 5) \tag{9}$$

The coefficients in Eq. (9) are very close to the number from 2-step resonance model, Eq. (8). When this straight line is extrapolated down to N=2, it corresponds to a depletion peak at Li-7. The big-bang theoretician may like this Li-7 depletion peak, because the observed Li-7 abundance in the early universe is lower than the predicted value [15] using the Bethe's non-resonance theory.

6. Where is the Gamma Radiation?

In Bethe's 2-step model, there is Gamma radiation in the second step, because the positron would annihilate with an electron to emit 2 Gamma photons. This positron was produced in a weak interaction,

$$p \rightarrow n + e^{+} + neutrino, \tag{10}$$

when the initial p+p elastic scattering state transited to a final (p+n) bound state. In 1935, Bethe was dealing with high temperature plasma in the sun (~1.5 keV). In the fully ionized plasma, there is no orbital electron around a proton.

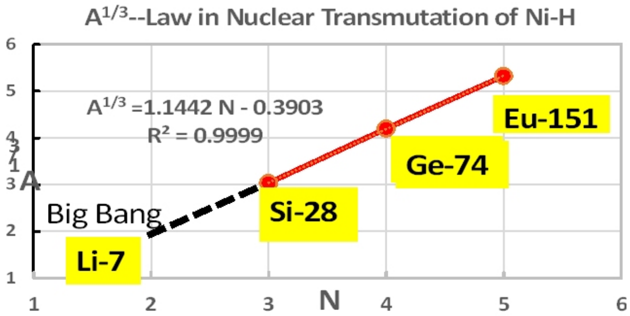

Figure 5. 3 depletion peaks support $\sqrt[3]{A}-$ law and 2-step resonance model.

Therefore, the positron emission was the only weak interaction to change a proton into a neutron and leads to Gamma radiation. However, when the 2-step resonance model is applied to low temperature nuclear transmutation ($\leq$ 1 eV) there will be another favorable weak interaction available to change a proton into a neutron. That is the K-electron capture process:

$$p + e_K^- \to n + neutrino, \tag{11}$$

This K-electron capture process is much more favorable than the positron emission process because the energy deficit is less by more than 1 MeV. That is why no gamma radiation was detected in Miley's Ni-H thin film experiments.

7. The $\sqrt[3]{\mathbf{A}}$ - Law in Electron Screening Data

As the name suggests, "electron screening effect" means an effect due to electron. However, the 5-peak pattern in "electron screening effect" (Fig. 6) and the 2-step resonance model may reveal the nuclear nature of the "electron screening effect". When 2-step resonance model is applied to the case of low energy nuclear reaction induced by deuteron, i.e.

$$d +_A^Z M_{\rm sc} \to p +_{A+1}^{\ \ Z} M \tag{12}$$

The 5-peak pattern may appear again as a result of the resonance in the $d +_A^Z M_{\rm sc}$ elastic scattering between deuteron and the deuterated screening metal $_A^Z M_{\rm sc}$.

Starting from the early days of this research, the "electron screening effect" has been applied to explain the deviation from the Gamow suppression, because the cross-section does not decrease with the deuteron energy (E) as steep as $e^{-\frac{\rm constant}{\sqrt{E}}}$. The possible physics behind this behavior was first attributed to the electron surrounding the nucleus. The orbital electrons might screen the positive nuclear charge, and it is equivalent to an acceleration of the incoming deuteron. Electrical screening potential ($\rm U_{sc}$) has been introduced to quantify this acceleration. If the deuteron is accelerated by this screening potential, the deuteron energy would increase from E to E+ $\rm U_{sc.}$. Thus it reduces the Gamow suppression from $e^{-\frac{\rm constant}{\sqrt{E}}}$ to $\rm e^{-\frac{constant}{\sqrt{E+U_{sc}}}}$. U_{sc} may be found by fitting the experimental dada. However, the U_{sc} is sometimes much greater than the expected value from any theoretical model. Moreover, when U_{sc} was plotted against the charge number (Z) of the screening metal $_A^Z M_{\rm sc}$, the 5-peak pattern was even more puzzling. Well before ICCF-25, D. Nagel discovered that the 5 peaks in electron screening potential U_{sc} have similar feature as those in the nuclear transmutation of metal-hydrides [16]. In 2006 and 2020, K. Czerski [17] and J. Kasagi [18] noticed the 5-peak pattern in Z from Raiola group's work in 2006 [19]. Z is the atomic number of the target (the screening metal $_A^Z M_{\rm sc}$). However, in the resonance condition of the 2-step resonance model, Eq. (5) and (6), the nuclear radius, $a_0 = c_{\rm a}$ ($\sqrt[3]{A}$+1),

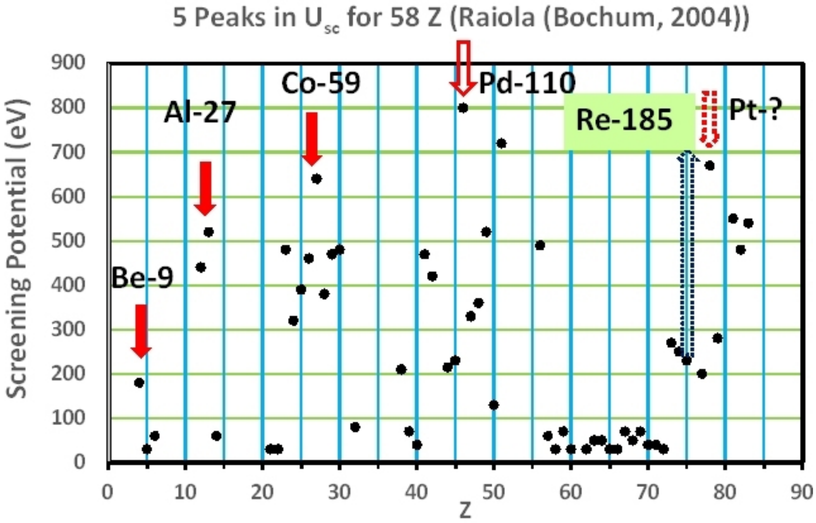

Figure 6. The screening potential for the 58 Z-numbers show 5 peaks as well [19].

depends on the atomic mass number, *A*, instead of atomic number, *Z*. In order to apply the 2-step resonance model, we have to find the *A* corresponding to 5 peaks in *Z* plot (indicated by 5 red downward arrows in Fig. 6). They are Be [4, 9], Al [13, 27], Co [27, 59], Pd[46, (102,104,105,106,108,110)], and Pt[78, (190,192,194,195,196,198)]. It is noticed that the first 3 peaks have only one stable isotope for each *Z* peak, but the last two peaks have 6 stable isotopes for each *Z* peak. How can we figure out the right *A* number for Pd and Pt? Our first attempt was to apply the $\sqrt[3]{A}$-law to the first 3 peaks; then, extrapolate the straight line to find the right isotope for Pd. It is a big surprise to find that Be, Al, and Co are just on a straight line (the red solid straight line in Fig. 6) with R^2= 0.99996.

$$\sqrt[3]{A_N} = 0.90270\ N + 1.18437.\ (N = 1,\ 2,\ 3) \tag{13}$$

Here A_N is the atomic mass number for the N-th peak. When Eq. (13) is extrapolated to N=4, it gives A_4 =110.8 which is close to Pd [46, 110].

The screening metal Pd in the Raiola's experiments was made of natural Pd. The natural abundance of Pd-110 is only 11.72%. Hence, we may expect that there would be a much higher peak in screening potential U_{sc} for an enriched Pd-110 screening metal. If this isotope effect is true, we may further suggest trying the screening experiment using an enriched Re-185 as the screening metal. We suppose we will observe the fifth peak at Re-185 (shown by the dotted upward black arrow in Fig. 6), instead of the peak at Pt (shown by the dotted downward red arrow in Fig. 6), because the natural abundance for Re-185 is only 34.70%. Fortunately, both Pd [46, 110] and Re [75, 185] are commercially available enriched isotopes (https://www.buyisotope.com/). The experimental equipment in Czerski's laboratory is already available for these tests. The only change needed is to replace the natural Pd and Re by the enriched Pd [46, 110] and Re [75, 185]. If Raiola's laboratory, Kasagi's laboratory and Hubler's laboratory are able to do the same electron screening experiment with the enriched Pd [46, 110] and Re [75, 185], and verify this isotope effect, then the assumption of nuclear nature of the 5-peak pattern in Nagel's discovery would be verified. It implies that same *Z* with a different *A* would have a different U_{sc}, i.e., there must be something other than the electron screening.

The possible explanation is: the thin screening metal film was loaded with deuterium during Raiola's screening experiments. The deuterated metals ${}^{Z}_{A}M_{sc}$ in these experiments provided not only the electrons to screen the fusion reaction d(d, p)t, but also the elastic scattering between $d +_A^Z M_{\rm sc}$. The resonance between $d +_A^Z M_{\rm sc}$ may deliver the deuteron to the surface of the nucleus $_A^Z M_{\rm sc}$ (the resonant pull-in effect), and the polarized deuteron may feed a neutron to the nucleus $_A^Z M_{\rm sc}$. This resonance induced stripping reaction $d +_A^Z M_{\rm sc} \to p +_{A+1}^{\ \ Z} M$ may yield the additional proton. In Raiola's experiments, the protons were counted to calculate the cross-section of the fusion reaction d(d, p)t. When this additional proton from the resonance stripping reaction is no longer negligible, it will increase the screening potential U_{sc}, and form the 5-peak pattern in $U_{sc} \sim Z$ plot.

If this is confirmed; then, the $\sqrt[3]{A}-$ law in electron screening data would be a strong support for the existence of the low energy nuclear resonance in condensed matter nuclear science using the hot fusion experiments.

8. Summary

When Bethe's solar energy model is extended to the case of resonance at low energy, the 2-step resonance model is proposed. It is able to explain both the temperature (T) dependence in excess power and the atomic mass number (A)-dependence in LENR of metal-hydrides. It may reveal further the isotope effect on the 5-peak pattern in electron screening data as well if the proposed experiments provide the affirmative results in enriched screening metals.

$\sqrt[3]{A}$-law in nuclear transmutation of metal-hydrides might be a key to find the regularity of LENR phenomena and to find a nuclear energy without strong nuclear radiation.

Acknowledgements

Many thanks to D. Nagel, G. Miley, T. Passell, F. Will, and J. Rothwell for their important assistance.

References

[1] X. Z. Li, et al., Resonant surface capture model, *J. Condensed Matter Nuclear Sci*. 29 (2019) 440–452.
[2] S. X. Zheng, et al., Temperature Dependence of Maximum Excess Power in 3 New Experiments (Letts, Parkhomov, & Mizuno), Abstract submitted to ICCF-22 (2019).
[3] X. Z. Li, et al. $A^{\frac{1}{3}}$—Law in Nuclear Transmutation of Metal Hydrides, Abstract submitted to ICCF-24 (2022).
[4] D. J. Nagel, Experimental Status of LENR, *ARPA-E Workshop on Low-Energy Nuclear Reactions*, p.16, 21-22 October 2021.
[5] H. A. Bethe, and C. L. Critchfield, The formation of deuterons by proton combination, *Phys. Rev*. **54** (1938) 248–254.
[6] National Nuclear Data Center, Brookhaven National Laboratory, ENDF/B-VIII.0 (2018) is available on Internet http://www.nndc.bnl.gov.
[7] X.Z. Li, J. Tian, M.Y. Mei and C.X. Li, Sub-barrier fusion and selective resonant tunneling, *Phys. Rev.* C **61** (2000) 024610.
[8] X.Z. Li, Nuclear Physics for Nuclear *Fusion, Fusion Science and Technology*, **41** (2002), 63–68.
[9] X.Z. Li, Q.M. Wei and B. Liu, A new simple formula for fusion cross-sections of light nuclei, *Nucl. Fusion* **48** (2008) 125003.
[10] C.L. Liang, X.Z. Li, Selective resonant tunneling – turning hydrogen storage material into energetic material, *Current Science*, **108**, No. 4, (2015) 519–523.
[11] E. Storms, How basic behavior of LENR can guide a search for an explanation, *J. Condensed Matter Nucl. Sci*. **20** (2016) 100–138.
[12] M. Abramowitz and I. A. Stegun, *Handbook of Mathematical Functions*, 10th Printing, December, 1972, p. 542. (14.6.9).
[13] P. E. Hodgson, The nuclear optical model, *1971 Rep. Prog. Phys*. **34**, 792.
[14] G. H. Miley and J.A. Patterson, Nuclear transmutations in Thin-Film Nickel Coatings Undergoing Electrolysis, *Journal of New Energy*, Vol. **1** (3) (1996) 5–13.
[15] C. Keeton. Principles of Astrophysics, ISBN 978-1-4614-9235-1, Springer New York Heidelberg Dordrecht London (2014), p. 408.
[16] D. J. Nagel, Potential Correlations between Apparent Peaks in LENR Transmutation Data and Deuteron Fusion Screening Data, *Pre-Print for ICCF-25 proceedings*, June 17, 2023.

[17] K. Czerski et al., Experimental and theoretical screening energies for the $^{2}H(d,p)^{3}H$ reaction in metallic environments, *European Physics Journal*, vol. **A 27**, s01, pp. 83–88 (2006).
[18] J. Kasagi et al., Screening Energy for Low Energy Nuclear Reactions in Condensed Matter, in J-P. Biberian (Editor), "*Cold Fusion: Advances in Condensed Matter Nuclear Science*", Elsevier, pp. 167–187 (2020).
[19] F. Raiola, et al., Enhanced d(d, p)t fusion reaction in metals, *Eur. Phys. J.* **A** 27, s01, 79–82 (2006).
[20] Book D. L. 1980 *NRL Plasma Formulary* (Washington DC: Naval Research Laboratory) p. 44, revised, and 2019 *NRL Plasma Formulary,* p. 44.

Appendix A. The Energy Dependence of the Phase-Shift in Low Energy Nuclear Fusion Reaction

The energy dependence of the phase-shift, $\mathrm{Cot}\,[\delta] = \theta^2(C_1 + C_2E)$,(i.e., Eq. (A.2)), plays an important role in extending Bethe's solar energy model to the case of low energy resonance. Indeed, this energy dependence is extracted from the fitting Eq. (A.1) with hot fusion data.

In 1999, $\mathrm{Cot}\,[\delta] \equiv W_r + i\,W_i$ was first introduced in a new simple formula to describe the low energy nuclear resonance [7], i.e.

$$\sigma_{\mathrm{fusion}} = \frac{\pi}{k^2}\frac{-4W_i}{W_r^2 + (1 - W_i)^2}, \tag{A.1}$$

Here, k is the wave number of the relative motion in the CM system, W_r and W_i are the real and imaginary part of $\mathrm{Cot}\,[\delta]$. This new formula is based on first principles, and is different from the famous Breit-Wigner formula which was written as a phenomenological formula. This new formula provides a bridge to extend the Bethe's non-resonance model to the 2-step resonance model using Eq. (1) and (2). Eq. (1) gives the T-dependence of reaction rate $<\sigma v>$ due to the low energy nuclear resonance, and Eq. (2) gives the 5-peaks in A-dependence of the production rate in the nuclear transmutation of metal-hydrides. In addition, Eq. (A.1) provides a tool to find the energy dependence of phase-shift from the experimental cross-section data.

In 2008 the 3-parameter formula was first proposed to fit 3 major fusion cross-section using $\mathrm{Cot}\,[\delta] = \theta^2(C_1 + C_2E + i\,C_3)$ and published by IAEA nuclear fusion journal [9]. Since 2008 it was cited by the handbook, "*NRL Plasma Formulary*" [20]. It was further applied to 8 pairs of fusion cross section in 2015 [10]. Now it is applied to 24 pairs of fusion cross-section successfully. This 3-parameter formula is:

$$\sigma_{\mathrm{Fusion}} = \frac{2609}{m_a}\left(1 + \frac{m_a}{m_b}\right)^2 \frac{1}{E_{\mathrm{lab}}}\left\{\frac{(-C_3)}{\theta^2\left[(C_1 + C_2E_{\mathrm{lab}})^2 + \left(C_3 - \frac{1}{\theta^2}\right)^2\right]}\right\}; \tag{A.2}$$

Here, E_{lab} is the incident energy in the laboratory system in keV, and σ_{Fusion} is in barns. m_a and m_b are the mass numbers of the injected projectile and target nucleus, respectively.

$$\theta = \sqrt{\frac{e^{31.4\, z_a z_b \sqrt{\frac{m_a}{E_{\mathrm{lab}}}}} - 1}{2\pi}}; \tag{A.3}$$

Three parameters, C_1, C_2, and C_3, for 24 fusion reactions are given in Table 1 using the least square fitting to experimental data from National Nuclear Data Center. Fig. A1-Fig. A24 show the comparison between 3-parameter formula and experimental data. These plots are drawn in both semi-logarithmic scale (the left vertical axis) and linear scale (the right vertical axis) in order to show clearly the comparison at both low and high energy region. The red solid lines show the 3-parameter formula's calculation, and the black circles show the experimental data points. Thus the real part of $\mathrm{Cot}\,[\delta]$ may be approximated by $\theta^2(C_1 + C_2E)$ in the case of elastic scattering.

This energy dependence of the phase-shift, $\mathrm{Cot}\,[\delta] = \theta^2(C_1 + C_2E + i\,C_3)$, is useful to predict the low energy behavior of the fusion cross-section. It was applied to d+T fusion and corrected a mistake in National Nuclear Data Center early in 1999 [8] for a d+T resonance peak at 100eV.

This energy dependence of the phase-shift, $\mathrm{Cot}\,[\delta] = \theta^2(C_1 + C_2E + i\,C_3)$, has solved an important question about the contribution from a low energy resonance also in terms of 2-step resonance. In the early days of cold fusion research, many scientists thought of the possible contribution from the low energy resonance; however, they were stopped by the width of the resonance. As the energy approaches zero, the Coulomb barrier becomes very thick, any

Table 1. C_1, C_2, and C_3 for 24 Pairs of Nuclear Fusion Reactions

No.	Reaction	C_1	C_2(keV^{-1})	C_3	Energy Range (keV)
1	p+D→Gamma+He3	$-6.4412\text{x}10^7$	$2.0484\text{x}10^6$	$-7.5499\text{x}10^7$	3.78–31.7
2	p+Li6→He3+He4	2.2331	$1.1116\text{x}10^{-3}$	-1.0853	1–880
3	p+Li7→2 He4	$-1.2185\text{x}10^2$	$7.4144\text{x}10^{-2}$	$-1.5921\text{x}10^2$	1.40–908
4	p+Be9→d+Be8	$-2.6622\text{x}10^{-2}$	$7.1440\text{x}10^{-5}$	$-3.9466\text{x}10^{-4}$	28–300
5	p+Be9→He4+Li6	$-4.4396\text{x}10^{-1}$	$1.4688\text{x}10^{-3}$	$-1.5989\text{x}10^{-1}$	13.4–320
6	p+B10→He4+Be7	$1.9639\text{x}10^{-2}$	$6.7023\text{x}10^{-5}$	$-1.1900\text{x}10^{-3}$	60–180
7	p+B11→He4+Be8	-4.9387	$2.9310\text{x}10^{-2}$	-2.4833	30–185
8	p+C13→G+N14	$-3.2321\text{x}10^2$	$5.8326\text{x}10^{-1}$	$-1.1403\text{x}10$	10–1000
9	d+d→n+He3	$-1.2261\text{x}10^2$	$1.2330\text{x}10^{-1}$	$-1.1074\text{x}10^2$	0.2–1000
10	d+d→p+T	$-1.3502\text{x}10^2$	$1.3131\text{x}10^{-1}$	$-1.3533\text{x}10^2$	0.2–1000
11	d+T→n+He4	$-5.4334\text{x}10^{-1}$	$5.5638\text{x}10^{-3}$	$-3.9021\text{x}10^{-1}$	0.2–280
12	d+He3→p+He4	$-9.8918\text{x}10^{-1}$	$2.7842\text{x}10^{-3}$	$-6.6483\text{x}10^{-1}$	0.9–1024
13	d+Li6→n+Be7	$1.2934\text{x}10^{-1}$	$3.1713\text{x}10^{-4}$	$-4.9996\text{x}10^{-2}$	3–500
14	d+Li6→p+Li7	$1.5363\text{x}10^{-1}$	$3.2286\text{x}10^{-4}$	$-5.5010\text{x}10^{-2}$	3–500
15	d+Li6→2 He4	$1.1204\text{x}10^{-1}$	$4.8175\text{x}10^{-4}$	$-3.6746\text{x}10^{-2}$	3–500
16	d+Li7→n+2 He4	$4.7198\text{x}10^{-3}$	$2.9463\text{x}10^{-6}$	$-4.8068\text{x}10^{-6}$	30.5–250
17	t+T→2 n+He4	$2.0208\text{x}10$	$4.3032\text{x}10^{-3}$	-7.2680	0.5–350
18	t+He3→n+p+He4	-8.4843	$2.6589\text{x}10^{-4}$	-9.4695	2–1000
19	t+He3→d+He4	4.4056	$1.5042\text{x}10^{-3}$	-1.0477	2–1000
20	t+Li6→n+2 He4	$4.1234\text{x}10^{-2}$	$8.5491\text{x}10^{-5}$	$-5.1430\text{x}10^{-2}$	20–400
21	t+Li6→d+Li7	$-4.8028\text{x}10^{-2}$	$2.1302\text{x}10^{-5}$	$-7.8243\text{x}10^{-3}$	20–900
22	He3+He3→2p+He4	1.0876	$8.2222\text{x}10^{-5}$	$-7.5157\text{x}10^{-1}$	51–2100
23	He3+Li6→p+2 He4	$-6.6425\text{x}10^{-4}$	$2.1730\text{x}10^{-6}$	$-4.0673\text{x}10^{-3}$	20–1000
24	He3+Li6→d+Be7	$-2.9573\text{x}10^{-2}$	$5.1993\text{x}10^{-5}$	$-9.4356\text{x}10^{-3}$	20–500

resonant tunneling effect would be damped by the nuclear fusion reaction itself in a 1-step model (damping effect to diminish a resonance due to $W_i = \theta^2 C_3 \ll -1$). Mathematically, the integration of a resonance in a 1-step model diminishes when the width of the resonance approaches zero. However, a 2-step resonance model assumes an elastic-scattering in the first step to fully develop a resonance without any damping ($W_i = 0$); then, the resonance will deliver the incoming projectile to the surface of the target, and greatly enhance the overlapping between the wave functions of the initial state and the final state. This is expressed by the term $\frac{1}{\sqrt{1+Cot[\delta]^2}}G_0$, in Eq. (1). This energy dependence of phase-shift Cot $[\delta] = \theta^2(C_1 + C_2 E) = \theta^2 C_2(E - E_0)$, in Eq. (2) make the transition probability of the second step, $\left|\frac{1}{\sqrt{1+Cot[\delta]^2}}G_0\right|^2 \propto \left|\frac{\theta}{\sqrt{1+(\theta^2 C_2(E-E_0))^2}}\right|^2$, a very sharp peak at the resonance $E = E_0$. The resonance peak height is proportional to θ^2, and the width of the resonance peak is proportional to $\frac{1}{\theta^2}$. When the energy approaches to zero, the width of the resonance becomes very narrow; however, the peak height of the resonance becomes very high accordingly. As a result, the integration of the resonance in a 2-step model is different from that of a 1-step model and is always not negligible. Mathematically the integration of a steep resonance may be calculated using the steepest descent method to give a finite value in a 2-step model.

In physics, the 1-step model is very different from the 2-step model. However, the physics of the 1-step model naturally leads to the development of the 2-step model. In 1-step model, the injected current of probability tunneling through Coulomb barrier region and penetrate the nuclear surface; then, the attenuated wave function would be absorbed there ($W_i \neq 0$). When the Coulomb barrier is very thick ($\theta^2 \gg 1$), the wave function is strongly attenuated by the barrier region. It needs a lot of bouncing back and forth motion inside the nuclear potential region to build up the wave function in order to have the resonance effect ($W_i \equiv \theta^2 C_3 \approx -\theta^2 \frac{\tau_{\text{bouncing}}}{\tau_{\text{life}}} = -1$, $\tau_{\text{bouncing}}$is the time scale for bouncing in the nuclear potential, τ_{life} is the life-time of the injected particle inside the nuclear potential [8]). However, if the absorption happens quickly ($\tau_{\text{life}} < \tau_{\text{bouncing}}$); then, the bouncing back and forth motion is stopped. There will be no chance to build up a resonance ($|W_i| = \left|\theta^2 \frac{\tau_{\text{bouncing}}}{\tau_{\text{life}}}\right| \gg 1, \sigma_{\text{fusion}} = \frac{\pi}{k^2}\frac{-4W_i}{W_r^2+(1-W_i)^2} \to 0$). Indeed, it is hardly possible to find a nuclear interaction to make $\frac{\tau_{\text{bouncing}}}{\tau_{\text{life}}} = \frac{1}{\theta^2}$; therefore, there is no way to have any resonant nuclear fusion reaction at low energy. Only the elastic scattering (The Rutherford scattering) remains at low energy ($\sigma_{\text{elastic}} = \frac{\pi}{k^2}\frac{4}{W_r^2+1}$). The resonance ($W_r = 0$) survives in the elastic scattering ($\sigma_{\text{elastic}\overrightarrow{W_{r=0}}}\frac{4\pi}{k^2}$), and it has a pull-in effect in addition to resonant tunneling. The resonance ($W_r = 0$) will make the wave function peak at the nuclear surface, and it will greatly enhance the overlapping between the initial state and final state wave functions. In this way, the integration of the resonance would not diminish in the 2-step resonance model while the integration of the resonance diminishes in the 1-step resonance model. The pull-in effect is a result of quantum (wave) mechanics. It is the key to understanding low energy nuclear resonance and condensed matter nuclear science.

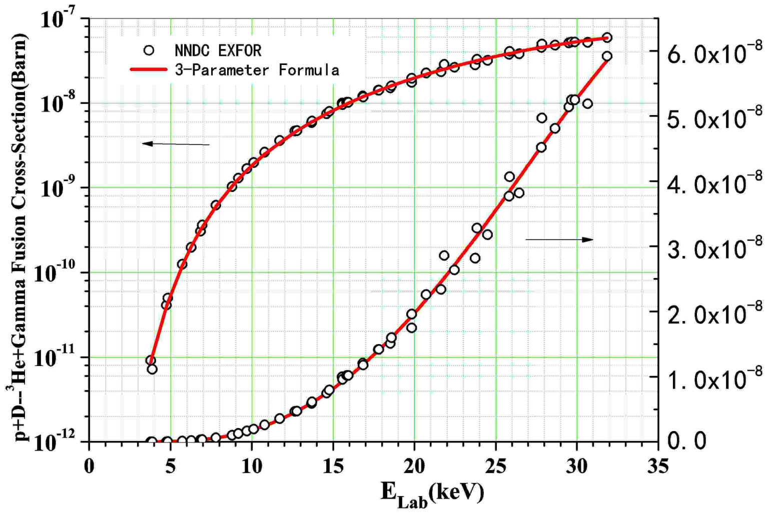

Figure A1. p+D→Gamma+He3.

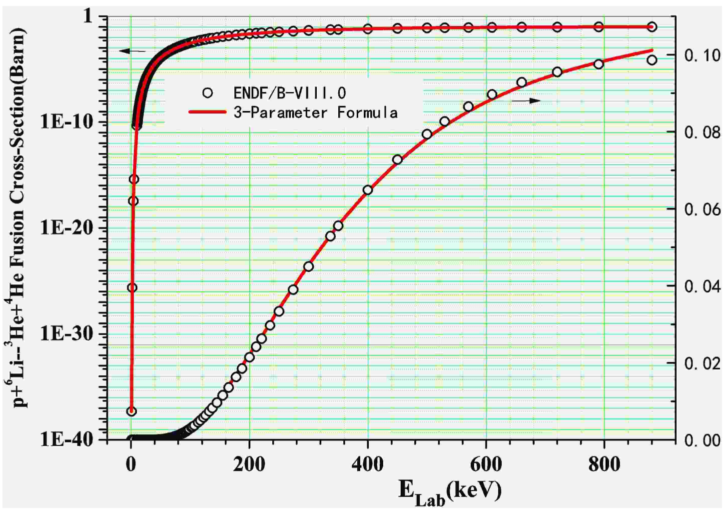

Figure A2. p+Li6→He3+He4.

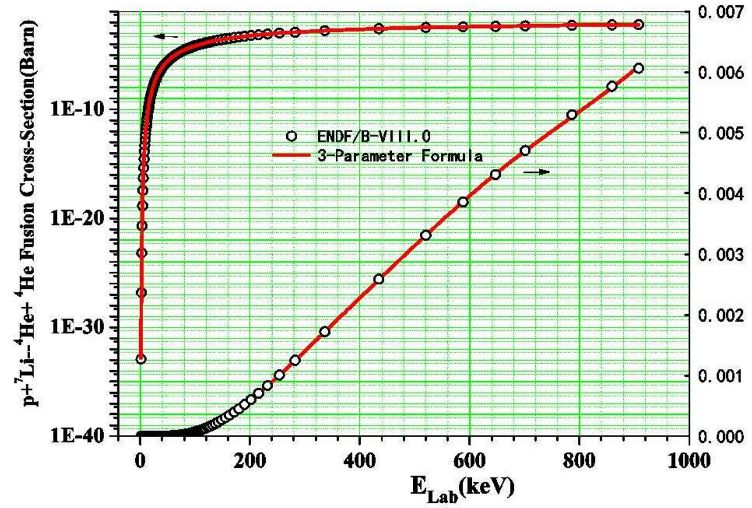

Figure A3. p+Li7→He4+He4.

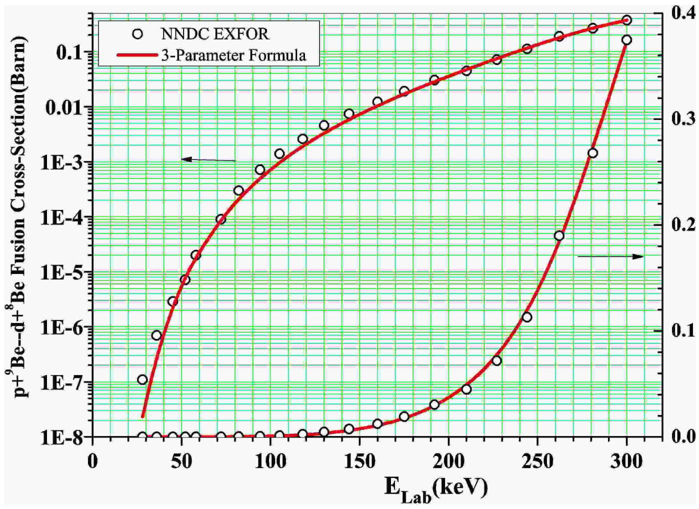

Figure A4. p+Be9→d+Be8.

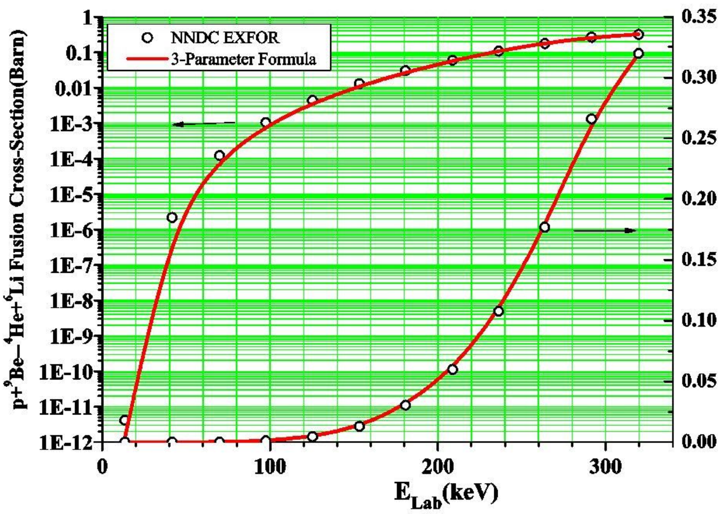

Figure A5. p+Be9→He4+Li6.

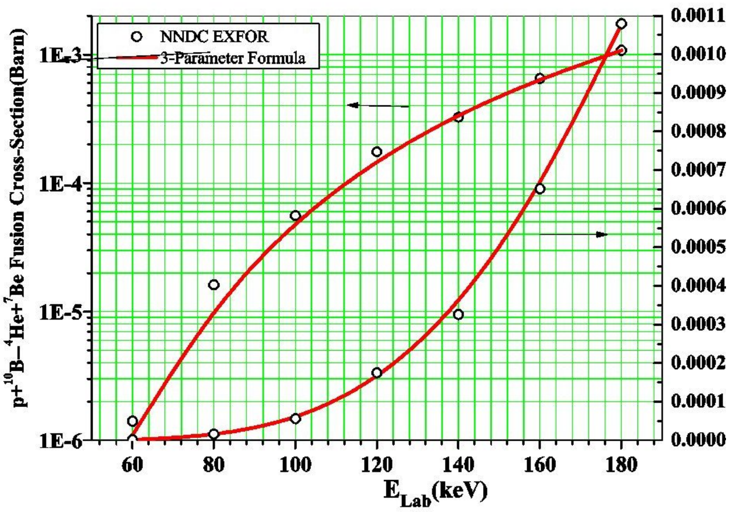

Figure A6. p+B10→He4+Be7.

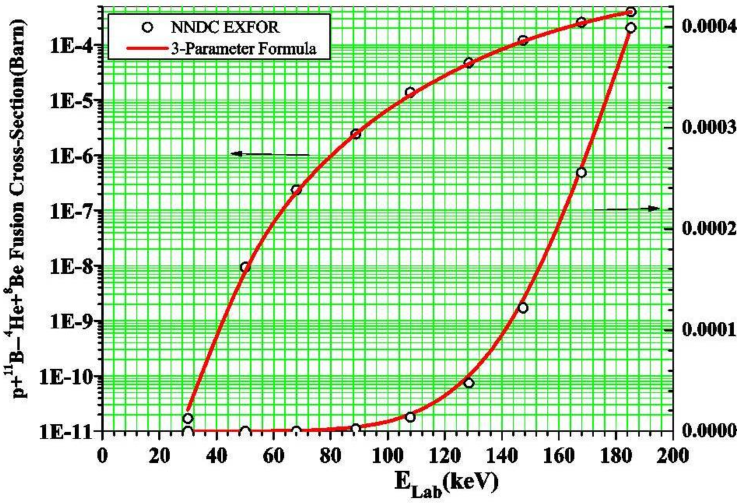

Figure A7. p+B11→He4+Be8.

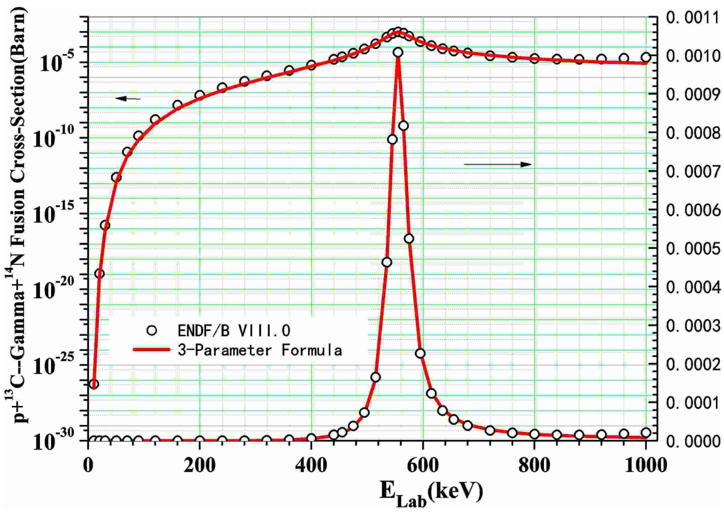

Figure A8. p+C13→Gamma+N14.

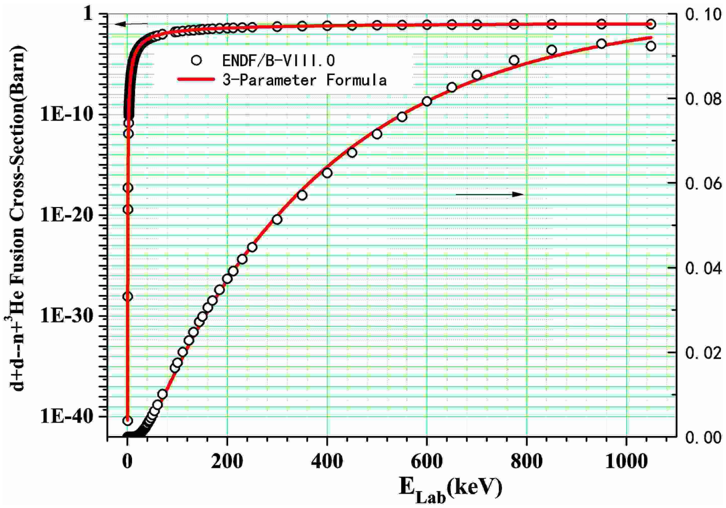

Figure A9. d+d→n+He3.

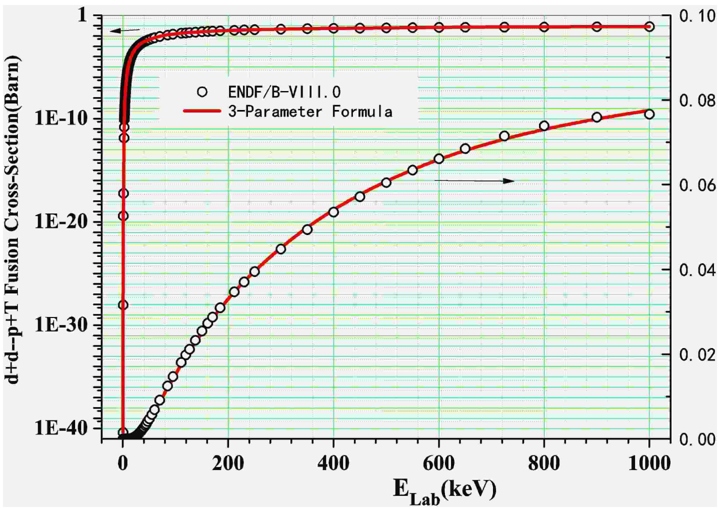

Figure A10. d+d→p+T.

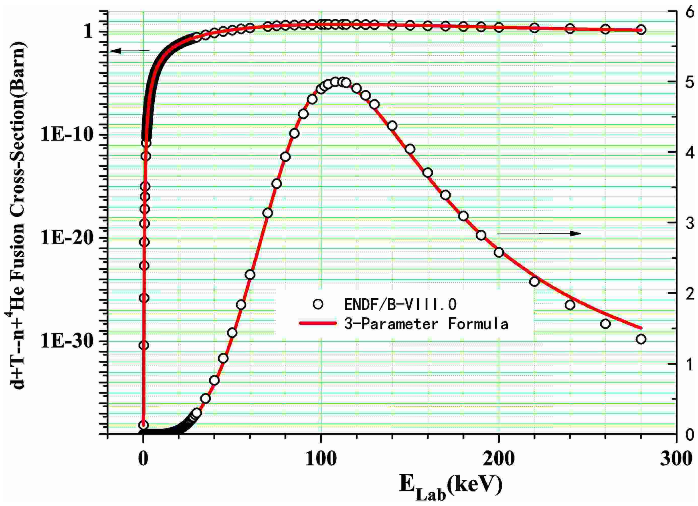

Figure A11. d+T→n+He4.

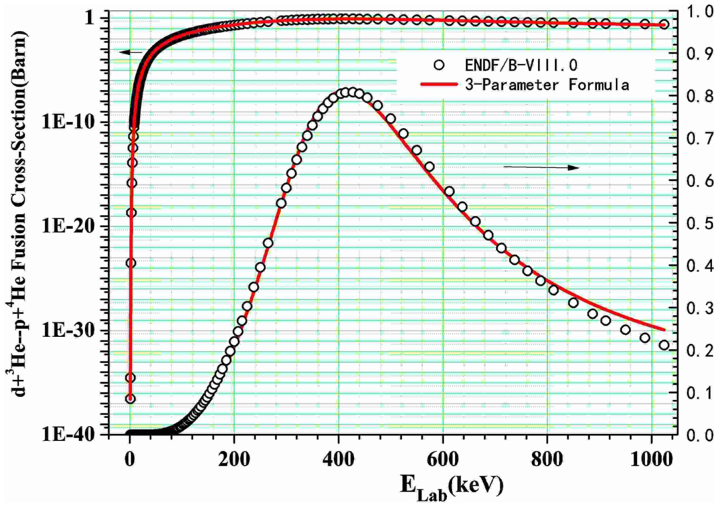

Figure A12. d+He3→p+He4.

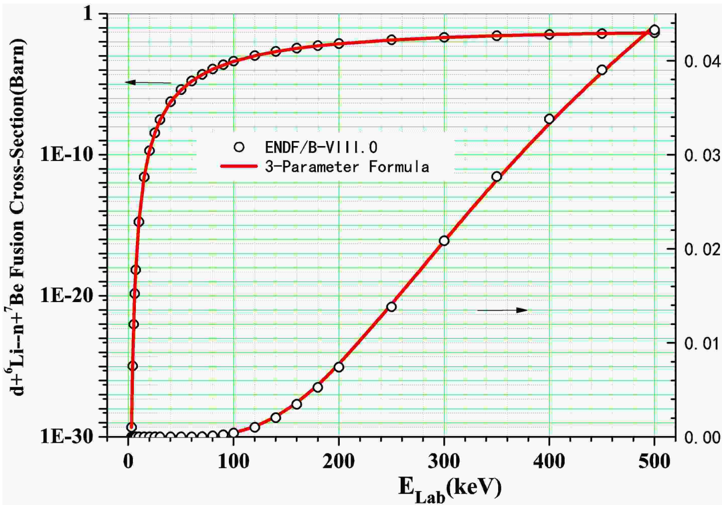

Figure A13. d+Li6→n+Be7.

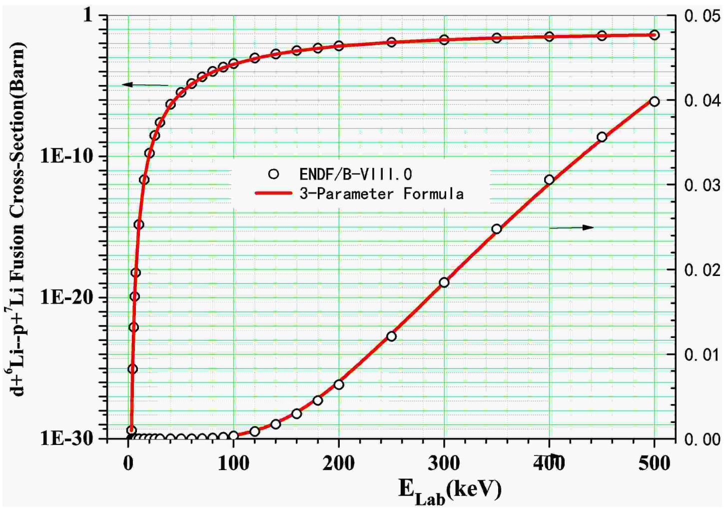

Figure A14. d+Li6→p+Li7.

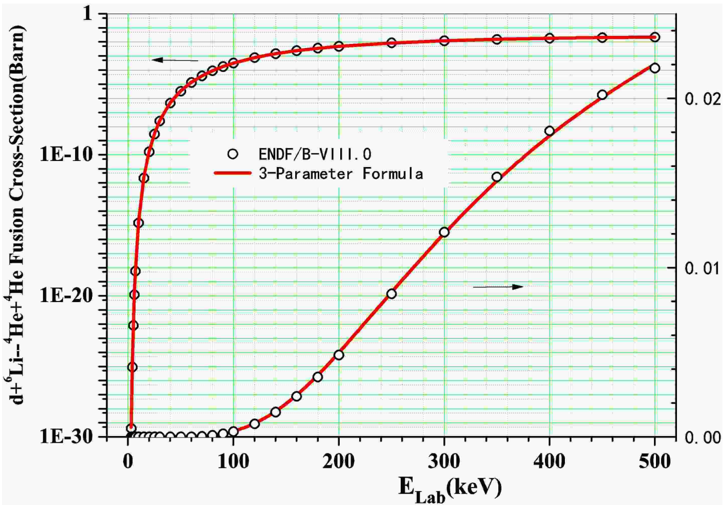

Figure A15. d+Li6→He4+He4.

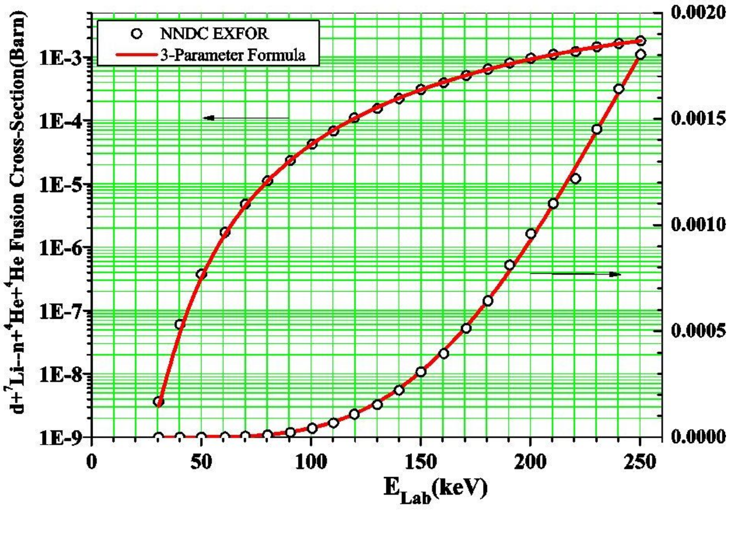

Figure A16. d+Li7→n+He4+He4.

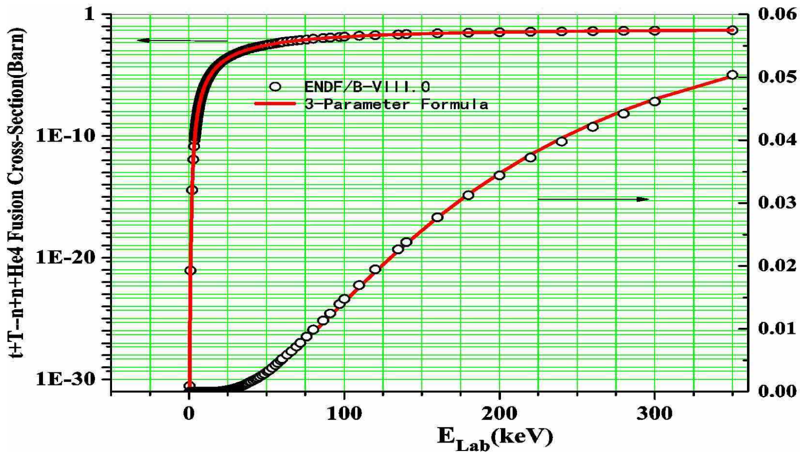

Figure A17. t+T→n+n+He4.

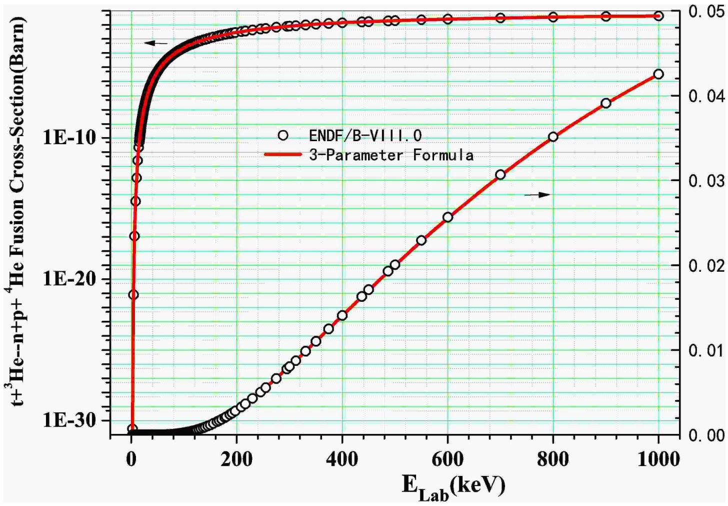

Figure A18. t+He3→n+p+He4.

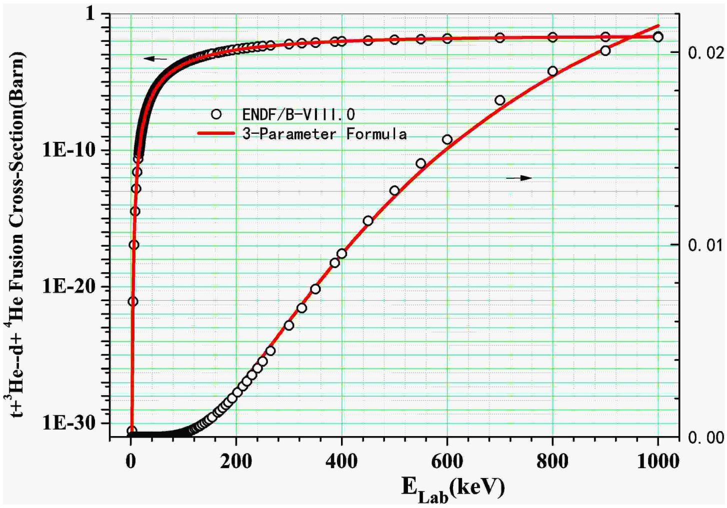

Figure A19. t+He3→d+He4.

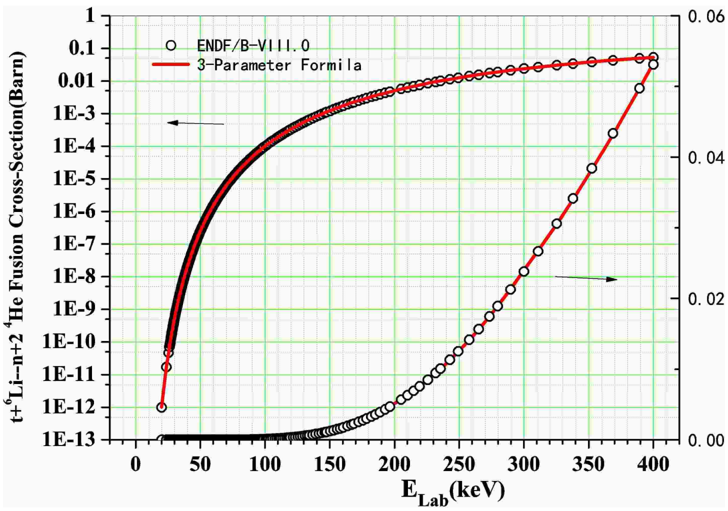

Figure A20. t+Li6→n+He4+He4.

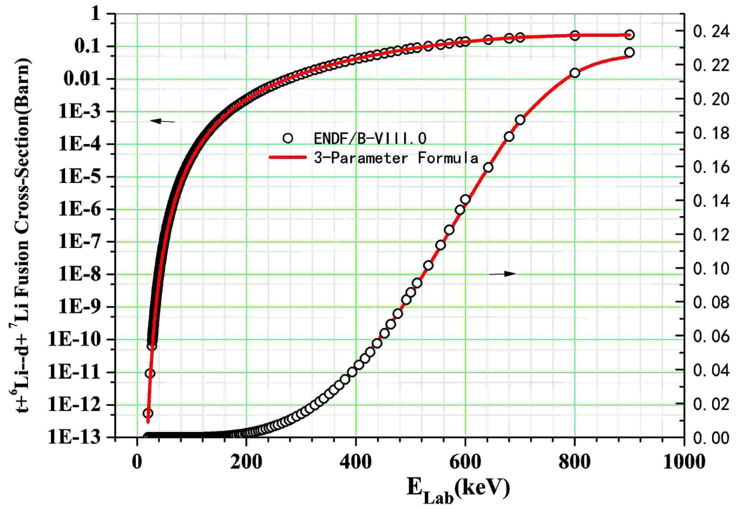

Figure A21. t+Li6→d+Li7.

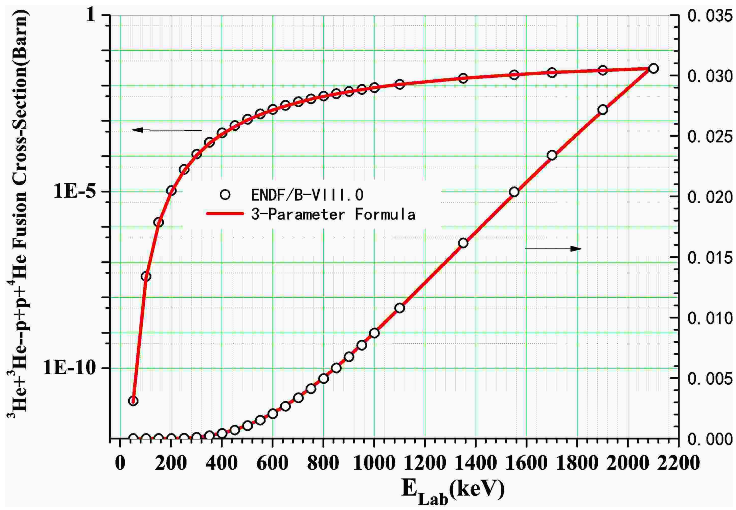

Figure A22. He3+He3→p+p+He4.

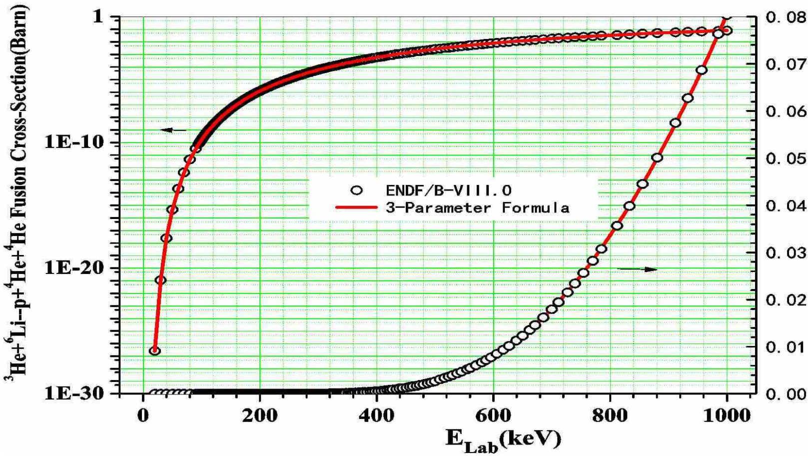

Figure A23. He3+Li6→p+He4+He4.

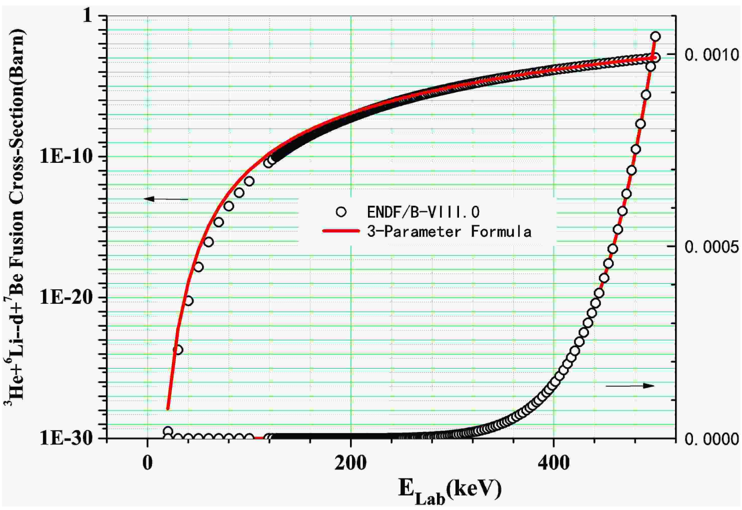

Figure A24. He3+Li6→d+Be7.